JACS
JOURNAL OF THE AMERICAN CHEMICAL SOCIETY
Communication
pubs.acs.org/JACS

Synthesis and Characterization of $[Ru@Ge_{12}]^{3-}$: An Endohedral 3-Connected Cluster

Gabriela Espinoza-Quintero, Jack C. A. Duckworth, William K. Myers, John E. McGrady,* and Jose M. Goicoechea*

Department of Chemistry, Inorganic Chemistry Laboratory, University of Oxford, Oxford, OX1 3QR, United Kingdom

Supporting Information

ABSTRACT: The 12-vertex endohedral cluster $[Ru@Ge_{12}]^{3-}$ reveals an unprecedented D_{2d}-symmetric 3-connected polyhedral geometry. The structure contrasts dramatically with the known deltahedral or approximately deltahedral geometries of $[M@Pb_{12}]^{2-}$ (M = Ni, Pd, Pt) and $[Mn@Pb_{12}]^{3-}$ and is a result of extensive delocalization of electron density from the transition-metal center onto the cage.

The chemistry of endohedral Zintl ion clusters has been developed extensively over the past decade.[1] Structurally characterized examples from the $[M@E_9]^{x-}$, $[M@E_{10}]^{x-}$, and $[M@E_{12}]^{x-}$ (x = 2, 3) families are now known[2−11] as well as a number of larger clusters where two transition-metal ions are encapsulated inside a main-group element cage.[12−15] The vast majority of these species are diamagnetic, their properties being readily understood in terms of a structurally inert d^{10} transition-metal atom/ion inside a *closo* deltahedral cage with a $4n + 2$ valence electron count. Within the 10-vertex family, the $[Ni@Pb_{10}]^{2-}$ cluster is a classic example, containing a formally zerovalent group 10 metal atom within a $[Pb_{10}]^{2-}$ cage.[4] However, the simultaneous reports of pentagonal prismatic $[Fe@Ge_{10}]^{3-}$ and $[Co@Ge_{10}]^{3-}$ in 2009 identified an alternative paradigm for $M@E_n$ clusters based not on deltahedral motifs but rather on 3-connected architectures.[5,6] In the absence of an endohedral metal, *closo*-deltahedral structures are characteristic of electron-deficient ($4n + 2$) electron counts while 3-connected structures are typical of electron-precise ($5n$) valence electrons. The preference for 3-connected structures in endohedral clusters of (relatively) early transition metals is therefore indicative of substantial transfer of electron density from the central metal to the E_{10} unit, i.e., the metal is far from inert in an electronic and structural sense. An intermediate case, $[Fe@Sn_{10}]^{3-}$, where the central metal is sufficiently electron-rich to induce significant distortions to the deltahedron but not to force the transition to a 3-connected polyhedron has also been identified recently.[7]

Turning to the 12-vertex family, the deltahedral structural type is exemplified by 60-electron icosahedral $[M@Pb_{12}]^{2-}$ (M = Ni, Pd, Pt) and $[Ir@Sn_{12}]^{3-}$, all of which can be understood as d^{10} metal atoms/ions inside deltahedral dianionic cages ($4n + 2 = 50$ electrons).[8−10] The 12-vertex analogue of $[Fe@Sn_{10}]^{3-}$ is $[Mn@Pb_{12}]^{3-}$, where the icosahedron is substantially distorted but still identifiably deltahedral.[11] Conspicuously absent, however, is a 12-vertex analogue of $[Fe@Ge_{10}]^{3-}$ and $[Co@Ge_{10}]^{3-}$, where the cluster adopts an entirely 3-connected geometry. In principle, the 12-vertex family offers three distinct 3-connected geometries, the hexagonal prism (D_{6h}), the T_d-symmetric truncated tetrahedron, and the D_{2d}-symmetric structure adopted by, the as of yet unidentified, $4^4{\cdot}5^4$ isomer of octahedrane ($C_{12}H_{12}$).[16]

Chart 1. Structures of Polyhedral Motifs in the 10- and 12-Vertex Families

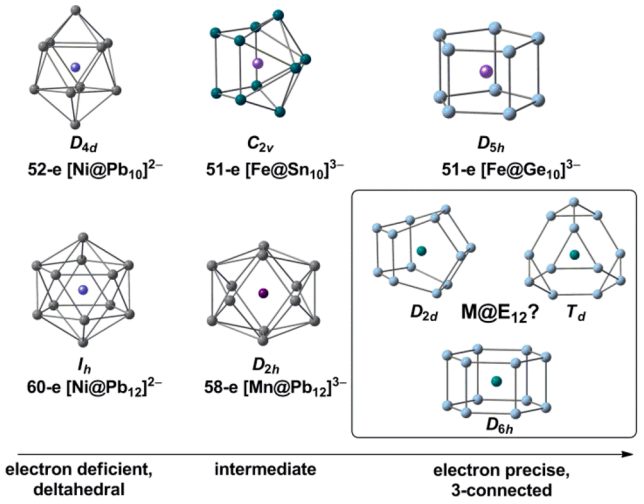

Structures of this type have been identified in a number of computational investigations of endohedral $M@Ge_{12}$ clusters and also for the empty Ge_{12} cages themselves.[17−22] For example, stable structures closely related to the hexagonal prism have been identified for $W@Ge_{12}$[17a] and $Os@Ge_{12}$[18] (as well as for the lighter silicon analogue $Cr@Si_{12}$).[23] The D_{2d}-symmetric form, in contrast, was reported to be the most stable isomer of $M@Ge_{12}$ where M is Ni,[17b,19] Cu,[20a] or Au.[20b] King et al. have also identified the D_{2d}-symmetric structure as an unstable isomer on the potential energy surface of the neutral empty Ge_{12} cage.[21] The truncated tetrahedral structure has been discussed by Schleyer and co-workers in the context of endohedral hydrocarbon cages.[24] Our previous experience with endohedral germanium clusters suggested that one of these 3-connected structures should be accessible (albeit synthetically challenging) with electron-rich transition metals. Herein, we report the synthesis and structural characterization of $[Ru@Ge_{12}]^{3-}$, which adopts the third of these 3-connected geometries (D_{2d}). It

Received: November 5, 2013
Published: December 30, 2013

   dx.doi.org/10.1021/ja411280v | J. Am. Chem. Soc. 2014, 136, 1210−1213

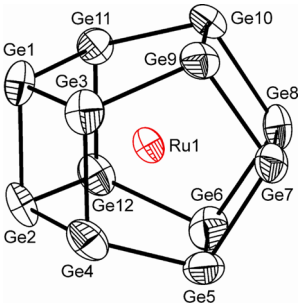

Figure 1. Molecular structure of the anionic cluster characterized in $[K(2,2,2\text{-crypt})]_3[Ru@Ge_{12}]\cdot 4py$ (anisotropic displacement ellipsoids pictured at 50% probability level). Minor disorder component (28% occupancy) has been removed for clarity. Selected bond distances (Å): Ru1–Ge1: 2.771(1); Ru1–Ge2: 2.735(1); Ru1–Ge3: 2.713(1); Ru1–Ge4: 2.675(1); Ru1–Ge5: 2.684(1); Ru1–Ge6: 2.667(2); Ru1–Ge7: 2.725(1); Ru1–Ge8: 2.721(1); Ru1–Ge9: 2.708(1); Ru1–Ge10: 2.705(2); Ru1–Ge11: 2.714(1); Ru1–Ge12: 2.651(1); Ge1–Ge2: 2.442(2); Ge1–Ge3: 2.489(2); Ge1–Ge11: 2.489(2); Ge2–Ge4: 2.479(2); Ge2–Ge12: 2.474(2); Ge3–Ge4: 2.577(2); Ge3–Ge9: 2.466(2); Ge4–Ge5: 2.466(2); Ge5–Ge6: 2.601(2); Ge5–Ge7: 2.485(2); Ge6–Ge8: 2.478(2); Ge6–Ge12: 2.467(2); Ge7–Ge8: 2.451(2); Ge7–Ge9: 2.485(2); Ge8–Ge10: 2.487(2); Ge9–Ge10: 2.599(2); Ge10–Ge11: 2.478(2); Ge11–Ge12: 2.585(2).

constitutes the first example of an endohedral complex of a 12-vertex Zintl cluster based on a 3-connected polyhedron and completes the 12-vertex family. Its electronic structure also reinforces the active structural role played by the d orbitals of the early/mid transition metals in clusters of this type.

The $[Ru@Ge_{12}]^{3-}$ anion was synthesized by reaction of an ethylenediamine solution of K_4Ge_9 with $[Ru(COD)\{\eta^3\text{-}CH_3C(CH_2)_2\}_2]$ (COD = 1,5-cyclooctadiene).[25] Multiple reactions were monitored by electrospray ionization mass-spectrometry (ESI-MS) in an attempt to find the optimal reaction conditions. Ultimately, we found that mild heating of the reaction mixture to 65 °C improved the yield of $[Ru@Ge_{12}]^{3-}$ and reduced the number of undesired side-products (specifically, eliminating the presence of $[Ge_9]^{x-}$ where x = 2–4). However despite these efforts, a compositionally pure sample of the cluster could not be obtained: dark greenish brown crystals of $[K(2,2,2\text{-crypt})]_3[Ru@Ge_{12}]\cdot 4py$ were found to crystallize alongside orange crystals of the known diamagnetic Zintl ion $[Ge_5]^{2-}$ (present in ESI-MS solutions of the crude reaction mixtures).[26] The different crystal morphologies and colors do, however, allow for a mechanical separation of the samples.[27] $[K(2,2,2\text{-crypt})]_3[Ru@Ge_{12}]\cdot 4py$ crystallizes in space group $P2_1$ (no. 4) and reveals a single crystallographically unique cluster anion in the asymmetric unit alongside three charge-balancing $[K(2,2,2\text{-crypt})]^+$ cations and some solvent of crystallization. Despite some issues with rotational disorder at the cluster site (see Supporting Information, SI, for full details) it is apparent from the crystal structure that the anion adopts an unprecedented D_{2d} geometry reminiscent of $4^4{\cdot}5^4$ octahedrane (Figure 1). Attempts to crystallize $[Ru@Ge_{12}]^{3-}$ using alternative sequestering agents or solvents were unsuccessful.

The 12-vertices of the D_{2d}-symmetric cage separate into two symmetry-distinct types, Ge_a (Ge1–2, 7–8) and Ge_b (Ge3–6, 9–12) in a 4:8 ratio. Each vertex is bonded to three adjacent atoms, giving a total of 18 edges. The pseudospherical nature of the cluster is reflected in the narrow distribution of Ru–Ge distances which vary between 2.651(1) and 2.771(1) Å, the longest of these corresponding to those between the endohedral metal and the atoms of the Ge_a set. The Ge–Ge distances range between 2.442(2) and 2.601(2) Å and are relatively short compared to the parent cluster anion (e.g., $[Ge_9]^{3-}$: 2.494(7)–2.713(7) Å),[28] but very similar to those reported for other three connected germanium clusters ($[Fe@Ge_{10}]^{3-}$: 2.526(1)–2.622(1) Å; $[Co@Ge_{10}]^{3-}$: 2.502(1)–2.622(1) Å).[5,6] The bond lengths are also comparable to the sum of the covalent single bond radii for two germanium atoms (2.40, 2.42 Å).[29]

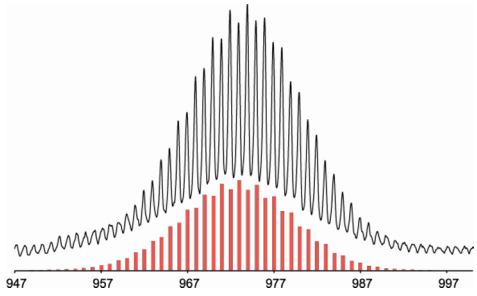

Figure 2. Negative ion-mode electrospray mass-envelope corresponding to $[Ru@Ge_{12}]^-$. Recorded experimental data are given in black with the calculated isotopic distribution in red.

The elemental composition of the cluster anion was confirmed by ESI-MS studies on DMF solutions of the crystalline product from which $[K(2,2,2\text{-crypt})]_3[Ru@Ge_{12}]\cdot 4py$ was isolated. Cluster peaks appear as distinct mass envelopes due to the variety of naturally occurring germanium (70, 72–74, 76) and ruthenium (96, 98–102, 104) isotopes, which allows for the unequivocal assignment of cluster-based signals.[30] As is often the case with the negative ion mode ESI-MS spectra of anionic Zintl ions, the clusters are observed with reduced charges as a result of the oxidation of the parent clusters during ionization/desolvation. The negative ion mode spectrum revealed mass envelopes corresponding to $[Ru@Ge_{12}]^-$ (Figure 2) and $\{[K(2,2,2\text{-crypt})][Ru@Ge_{12}]\}^-$ at m/z values of 973.9 and 1389.2, respectively. Positive ion mode spectra also revealed a peak corresponding to $\{[K(2,2,2\text{-crypt})]_4[Ru@Ge_{12}]\}^+$ at 2636.5 Da. Mass spectrometry further corroborated the presence of $[Ge_5]^{2-}$ as a reaction product (–ve ion mode: 364.0 $[Ge_5]^-$, 403.4 $\{K[Ge_5]\}^-$, 779.6 $\{[K(2,2,2\text{-crypt})][Ge_5]\}^-$; +ve ion mode: 1609.8 $\{[K(2,2,2\text{-crypt})]_3[Ge_5]\}^+$), confirming the nonstoichiometric nature of the reaction.

X-band CW-EPR measurements on a sample of $[K(2,2,2\text{-crypt})]_3[Ru@Ge_{12}]\cdot 4py$ at isotopic natural abundance in a pyridine glass confirm the paramagnetic character of the anion. The spectrum shown in Figure 3 can be simulated using axially anisotropic g values ($g_\parallel$ = 1.993, $g_\perp$ = 2.043) and an isotropic hyperfine coupling of $|A_{iso}|$ = 33 MHz on the eight symmetry-related Ge_b atoms.

To explore the origins of the highly unusual geometry adopted by the $[Ru@Ge_{12}]^{3-}$ anion, we have used density functional theory to compute the relative energies of various high-symmetry points on its doublet potential energy surface. The most stable minimum has D_{2d}-symmetry, and bond lengths very similar to those reported from the crystallographic experiment: Ru–Ge and Ge–Ge distances lie in the range 2.81–2.89 and 2.56–2.72 Å, respectively. The computed g factors ($g_\parallel$ = 2.000, $g_\perp$ = 2.023) for the D_{2d} structure are also very similar to those obtained from the simulation of the EPR data, as are the relative magnitudes of the computed isotropic hyperfine constants at Ge_a (3 MHz) and Ge_b (–20 MHz): only the former can be resolved in the measured spectrum ($|A_{iso}|$ = 33 MHz), as detailed in the SI. The

dx.doi.org/10.1021/ja411280v | J. Am. Chem. Soc. 2014, 136, 1210–1213

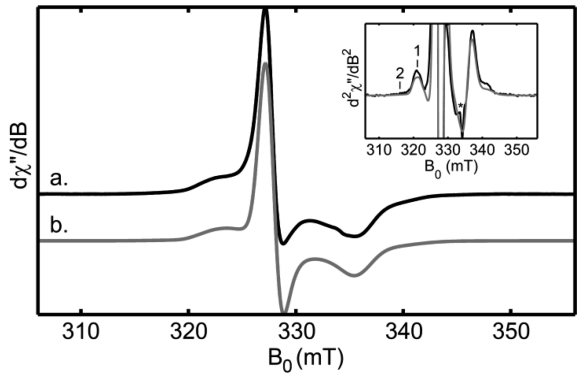

Figure 3. Experimental (a, black) and simulated (b, gray) EPR spectra for $[Ru@Ge_{12}]^{3-}$. The simulation uses $g_{\|} = 1.993$ and $g_{\perp} = 2.043$, with $|A(^{73}Ge_b)| = 33$ MHz given a Gaussian distribution of $\sigma = 20$ MHz. Inset: second derivative of absorption by pseudomodulation of the data and simulation, showing shoulders corresponding to one $^{73}Ge(1)$ and more than one $^{73}Ge(2)$ located in the eight Ge_b positions. Nonsaturating conditions were found at 85 K, with a microwave frequency of 9.3691 GHz, microwave power of 10 μW, modulation amplitude of 0.2 mT, a time constant of 81.92 ms, and a sweep rate of 42.94 s over 50 mT.

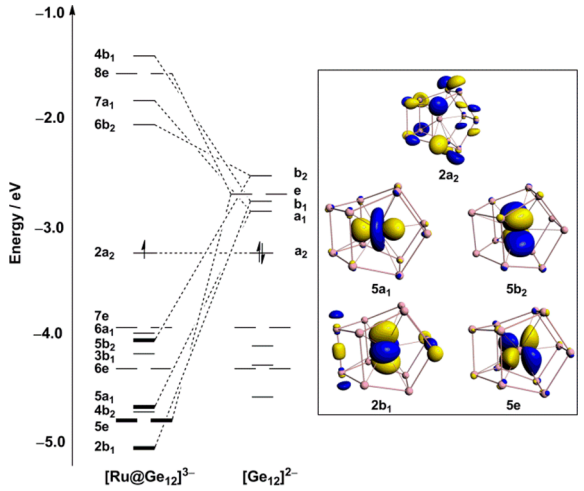

Figure 4. Frontier Kohn–Sham orbitals for D_{2d}-symmetric $[Ru@Ge_{12}]^{3-}$. Orbitals with dominant Ru contribution are shown in bold.

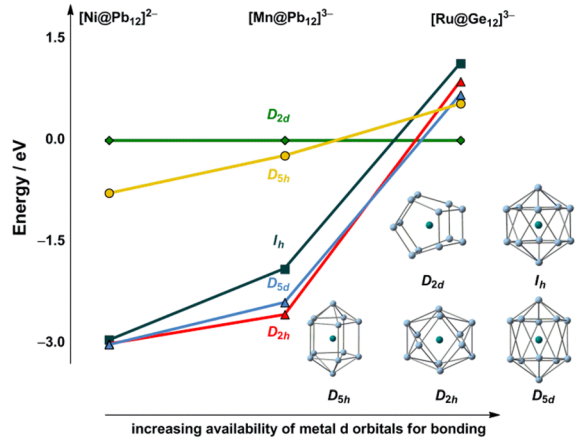

Figure 5. Relative energies of high-symmetry stationary points on the potential energy surfaces of representative members of the 12-vertex family. The D_{2d}-symmetric structure is taken as the energetic reference point for each cluster.

very different hyperfine coupling constants at Ge_a and Ge_b are at first glance surprising, given that the $2a_2$ SOMO shown in Figure 4 is delocalized over all 12 Ge centers, giving similar spin densities at Ge_a (0.073) and Ge_b (0.098). However, the Ge_a character in the SOMO is exclusively Ge 4p (by symmetry), while for Ge_b a substantial 4s contribution leads to a much larger contact coupling.

The alternative T_d- and D_{6h}-symmetric 3-connected isomers proposed in Chart 1 are 5.86 and 2.86 eV less stable, respectively, than the D_{2d}-symmetric minimum, and both have multiple imaginary frequencies. Among the approximately deltahedral structures (I_h, D_{5d}, D_{2h}), the D_{5d} isomer lies lowest and is only 0.68 eV above the equilibrium structure. This structure does not, however, correspond to a true minimum on the potential energy surface (nimag =1), and following the imaginary frequency leads to a D_{5h}-symmetric bicapped pentagonal prism at +0.55 eV. This isomer is a local minimum and has been identified in Tang et al.'s study of neutral $M@Ge_{12}$ (M = first-row transition metal),[22] but to the best of our knowledge has no precedent among structurally characterized species.

In order to place the new $[Ru@Ge_{12}]^{3-}$ anion in the broader context of the known structural chemistry of endohedral 12-vertex clusters, we have performed a similar survey of the potential energy surface for the known deltahedral anions $[Ni@Pb_{12}]^{2-}$ and $[Mn@Pb_{12}]^{3-}$; the results are summarized in Figure 5. The horizontal axis in Figure 5 maps out a progressive destabilization of metal d orbitals (Ni < Mn < Ru), and this correlates with a stabilization of the 3-connected D_{2d} isomer and, to a lesser extent, the D_{5h}-symmetric bicapped pentagonal bipyramid, relative to the approximately deltahedral alternatives (I_h, D_{5d}, D_{2h}). In both $[Ni@Pb_{12}]^{2-}$ and $[Mn@Pb_{12}]^{3-}$ the D_{2d}-symmetric structure is substantially *less* stable than either the perfect icosahedron or its D_{5d} or D_{2h}-symmetric distorted variants, entirely consistent with the crystallographic evidence. The defining role of the metal d orbitals in the structural chemistry is highlighted by simple electron counting principles which demand an electron precise count (i.e., $5n = 60$ valence electrons) for a 3-connected cage. This limit can be approached *only* if all 8 d electrons on Ru are included in the valence electron count along with 48 from the 12 Ge centers and 3 from the charge, giving 59 in total (see Table 1). The single 'hole' is entirely localized on the cage ($2a_2$ in Figure 4, $\rho(Ge_{12}) = 1.08$), while the Ru 4d character accumulates in a band of five doubly occupied orbitals, {$5b_2$, $5a_1$, 5e, $2b_1$} with significant bonding character, some 1–2 eV below the SOMO. Conversely, the approximately deltahedral (*closo*) structures (I_h, D_{5d}, D_{2h}) demand a $4n + 2 = 50$ valence electron count on the cage, which in turn requires that the metal d orbitals are *not* included in the count (i.e., they are structurally inert). This would imply a negative formal oxidation state, Ru(−I), consistent with the relatively high Mulliken spin densities on the metal in these isomers. Of course the transition from active to inactive metal d orbitals is not an abrupt one, and the series shown in Figure 5 maps out a structural continuum from perfectly icosahedral ($[Ni@Pb_{12}]^{2-}$) through distorted icosahedral ($[Mn@Pb_{12}]^{3-}$) to 3-connected ($[Ru@Ge_{12}]^{3-}$).

In this paper we have described the synthesis and crystallographic characterization of $[Ru@Ge_{12}]^{3-}$, an entirely new type of 12-vertex endohedral Zintl-ion cluster where the vertices are 3-connected. The cluster is the 12-vertex analogue of the pentagonal prismatic $[Fe@Ge_{10}]^{3-}$ and $[Co@Ge_{10}]^{3-}$. Density functional theory has then been used to place this new cluster in

dx.doi.org/10.1021/ja411280v | J. Am. Chem. Soc. 2014, 136, 1210–1213

Table 1. Optimized Bond Lengths and Total Energies (relative to D_{2d}) of Various Isomers of $[Ru@Ge_{12}]^{3-}$ [a]

	D_{2d}	D_{6h}	T_d	D_{5h}	I_h	D_{5d}	D_{2h}
Ru−Ge /Å	2.81−2.89	2.91	3.02	2.78−3.13	2.76	2.76−3.07	2.65−2.90
Ge−Ge /Å	2.56−2.72	2.56−2.61	2.52−2.62	2.70−3.14	2.91	2.72−3.35	2.71−3.07
ρ(Ru)	−0.08	0.17	−0.19	0.59	0.30	0.57	0.43
$\rho(Ge_{12})$	1.08	0.83	1.19	0.41	0.70	0.43	0.57
n_{imag}	0	6	12	0	5	1	1
E/eV	0.0	+2.86	+5.86	+0.55	+1.15	+0.68	+0.99

[a]Mulliken spin densities, ρ, on the Ru center and the cage are also shown, as is the number of imaginary frequencies (n_{imag}) in each case.

the context of the wider 12-vertex family (including perfectly icosahedral $[Ni@Pb_{12}]^{2-}$ and the distorted but still identifiably deltahedral D_{2h}-symmetric $[Mn@Pb_{12}]^{3-}$). The three clusters lie on a continuum defined by the electron richness of the metal: in $[Ni@Pb_{12}]^{2-}$ the d orbitals are low-lying and structurally inert, while in $[Ru@Ge_{12}]^{3-}$ all five are strongly mixed with vacant orbitals on the cluster. The 3-connected geometry characteristic of electron-precise clusters is optimal in this case because it allows all the five d orbitals of the electron-rich metal to participate in back-bonding, giving an effective 5*n* electron count at the cage.

■ ASSOCIATED CONTENT

Supporting Information

Experimental details and diffraction data. This material is available free of charge via the Internet at http://pubs.acs.org.

■ AUTHOR INFORMATION

Corresponding Author

jose.goicoechea@chem.ox.ac.uk; john.mcgrady@chem.ox.ac.uk

Notes

The authors declare no competing financial interest.

■ ACKNOWLEDGMENTS

We thank the Mexican Consejo Nacional de Ciencia y Tecnología (CONACYT; studentship G.E.Q.) and the University of Oxford for financial support of this research. We also thank the University of Oxford for access to OSC and CAESR facilities. Professor Paul R. Raithby (Bath) is also acknowledged for helpful discussions on the SXRD data.

■ REFERENCES

(1) Recent reviews: (a) Sevov, S. C.; Goicoechea, J. M. *Organometallics* **2006**, *25*, 5678. (b) Scharfe, S.; Fässler, T. F. *Phil. Trans. R. Soc. A* **2010**, *368*, 1265. (c) Scharfe, S.; Kraus, F.; Stegmaier, S.; Schier, A.; Fässler, T. F. *Angew. Chem., Int. Ed.* **2011**, *50*, 3630.

(2) Goicoechea, J. M.; Sevov, S. C. *J. Am. Chem. Soc.* **2006**, *128*, 4155.

(3) Scharfe, S.; Fässler, T. F.; Stegmaier, S.; Hoffmann, S. D.; Ruhland, K. *Chem.—Eur. J.* **2008**, *14*, 4479.

(4) Esenturk, E. N.; Fettinger, J.; Eichhorn, B. *Chem. Commun.* **2005**, 247.

(5) Zhou, B.; Denning, M. S.; Kays, D. L.; Goicoechea, J. M. *J. Am. Chem. Soc.* **2009**, *131*, 2802.

(6) Wang, J.-Q.; Stegmaier, S.; Fässler, T. F. *Angew. Chem., Int. Ed.* **2009**, *48*, 1998.

(7) Krämer, T.; Duckworth, J. C. A.; Ingram, M. D.; Zhou, B.; McGrady, J. E.; Goicoechea, J. M. *Dalton Trans.* **2013**, *42*, 12120.

(8) Esenturk, E. N.; Fettinger, J.; Lam, Y.-F.; Eichhorn, B. *Angew. Chem., Int. Ed.* **2004**, *43*, 2132.

(9) Esenturk, E. N.; Fettinger, J.; Eichhorn, B. *J. Am. Chem. Soc.* **2006**, *128*, 9178.

(10) Wang, J.-Q.; Stegmaier, S.; Wahl, B.; Fässler, T. F. *Chem.—Eur. J.* **2010**, *16*, 1793.

(11) Zhou, B.; Krämer, T.; Thompson, A. L.; McGrady, J. E.; Goicoechea, J. M. *Inorg. Chem.* **2011**, *50*, 8028.

(12) Goicoechea, J. M.; Sevov, S. C. *Angew. Chem., Int. Ed.* **2005**, *44*, 4026.

(13) Goicoechea, J. M.; Sevov, S. C. *J. Am. Chem. Soc.* **2005**, *127*, 7676.

(14) Kesanli, B.; Halsig, J. E.; Zavalij, P.; Fettinger, J. C.; Lam, Y.-F.; Eichhorn, B. W. *J. Am. Chem. Soc.* **2007**, *129*, 4567.

(15) (a) Sun, Z. M.; Xiao, H.; Li, J.; Wang, L.-S. *J. Am. Chem. Soc.* **2007**, *129*, 9560. (b) Kocak, F. S.; Zavalij, P.; Lam, Y.-F.; Eichhorn, B. W. *Inorg. Chem.* **2008**, *47*, 3515.

(16) (a) McGlinchey, M. J.; Hopf, H. *Beilstein J. Org. Chem.* **2011**, *7*, 222. (b) Wu, H.-S.; Qin, X. F.; Xu, X. H.; Jiao, H.; Schleyer, P. v. R. *J. Am. Chem. Soc.* **2005**, *127*, 2334.

(17) (a) Wang, J.; Han, J.-G. *J. Phys. Chem. A* **2006**, *110*, 12670. (b) Wang, J.; Han, J.-G. *J. Phys. Chem. B* **2006**, *110*, 7820.

(18) Lu, J.; Nagase, S. *Chem. Phys. Lett.* **2003**, *372*, 394.

(19) Bandyopadhyay, D.; Sen, P. *J. Phys. Chem. A* **2010**, *114*, 1835.

(20) (a) Wang, J.; Han, J.-G. *J. Chem. Phys.* **2005**, *123*, 244303. (b) Li, X.-J.; Su, K.-H. *Theor. Chem. Acc.* **2009**, *124*, 345.

(21) King, R. B.; Silaghi-Dumitrescu, I.; Uţă, M. M. *Dalton Trans.* **2007**, 364.

(22) Tang, C.; Liu, M.; Zhu, W.; Deng, K. *Comput. Theor. Chem.* **2011**, *969*, 56.

(23) (a) Khanna, S. N.; Rao, B. K.; Jena, P. *Phys. Rev. Lett.* **2002**, *89*, 016803. (b) Robles, R.; Khanna, S. *Phys. Rev. B.* **2009**, *80*, 115414. (c) Zheng, W.; Nilles, J. M.; Radisic, D.; Bowen, K. H. *J. Chem. Phys.* **2005**, *122*, 1.

(24) Moran, D.; Woodcock, H. L.; Chen, Z.; Schaeffer, H. F., III; Schleyer, P. v. R. *J. Am. Chem. Soc.* **2003**, *125*, 11442.

(25) K_4Ge_9 (80 mg, 0.1 mmol) and 2,2,2-crypt (110 mg, 0.3 mmol) were stirred in ethylenediamine (4 mL) for 5 min giving rise to a dark-brown solution. A THF (2 mL) solution of $[Ru(COD)\{\eta^3\text{-}CH_3C(CH_2)_2\}_2]$ (31 mg, 0.1 mmol) was added dropwise to the ethylenediamine solution. The mixture was stirred at 65 °C for 5 h and filtered. All volatiles were removed under reduced pressure to leave a brown powder which was washed with THF (10 mL). The resulting solid was dissolved in pyridine (5 mL) and filtered into an airtight ampule. Slow diffusion of toluene into the pyridine solution afforded dark-brown block-like crystals of $[K(2,2,2\text{-crypt})]_3[Ru@Ge_{12}]\cdot 4py$ after 2 weeks. This sample crystallized alongside orange block-like crystals of $[K(2,2,2\text{-crypt})]_2[Ge_5]$.

(26) Campbell, J.; Schrobilgen, G. J. *Inorg. Chem.* **1997**, *36*, 4078.

(27) Crystallographic data for $[K(2,2,2\text{-crypt})]_3[Ru@Ge_{12}]\cdot 4py$: monoclinic, $P2_1$ (no. 4), a = 14.1424(1) Å, b = 26.0428(2) Å, c = 14.2684(1) Å, β = 107.754(1)°, V = 5004.88(6) Å^3, Z = 2, T = 150(2) K, ρ_{calc} = 1.682 g cm^{-3}, μ = 6.790 mm^{-1}, *R*1/*wR*2 5.74/15.52% for the observed data ($I \geq 2\sigma(I)$), *R*1/*wR*2 6.15/16.21% for all the data, GOF = 1.022.

(28) Fässler, T. F.; Hunziker, M. *Inorg. Chem.* **1994**, *33*, 5380.

(29) (a) Pyykkö, P.; Atsumi, M. *Chem.—Eur. J.* **2009**, *15*, 186. (b) Cordero, B.; Gómez, V.; Platero-Prats, A. E.; Revés, M.; Echeverría, J.; Cremades, E.; Barragán, F.; Alvarez, S. *Dalton Trans.* **2008**, 2832.

(30) de Laeter, J. R.; Böhlke, J. K.; de Bièvre, P.; Hidaka, H.; Peiser, H. S.; Rosman, K. J. R.; Taylor, P. D. P. *Pure Appl. Chem.* **2003**, *75*, 683.